2.4 NANOSCALE 3D CORRELATIVE ATOM PROBE-ELECTRON TOMOGRAPHY: CHARACTERIZATION OF MICROSTRUCTURES IN DUAL ION IRRADIATED NFA MA957 — P. B. Wells, S. Krämer, Y. Wu, S. Pal, G. R. Odette and T. Yamamoto (University of California, Santa Barbara)

OBJECTIVE

The objective of this study is to use a combination of atom probe (APT) and 3D electron tomography (ET) to characterize nm-scale helium bubbles (HB) and nano-oxides (NO) in dual ion irradiated MA957 to characterize their mutual associations, as well as their associations with other microstructural features, such as grain boundaries.

SUMMARY

Transmission Electron Microscopy (TEM) can resolve very small helium bubbles (HB), down to approximately 1 nm, but is not optimal for observing populations of very small nano-oxides (NO) in nanostructured ferritic alloys (NFA). In contrast, atom probe tomography (APT) excels in measuring the location, size and composition of NO, but cannot resolve small bubbles. Because a typical APT tip has dimensions similar to those needed for TEM (on the order of 50-100 nm thickness), it is possible to characterize HB by 3D TEM tomography, hereafter called ET, prior to destructive 3D characterization of the NO by APT. Here, for the first time, APT and ET are used to assess the association between HB and NO in full 3D reconstructions, which also reveal strong NO-HB associations with a grain boundary.

BACKGROUND

Structural materials for use in fusion reactors must be able to withstand neutron doses in the hundreds of dpa and manage high concentrations of He generated in neutron-alpha reactions. Insoluble helium atoms cluster in steels to form nm-scale pressurized bubbles [1, 2]. When helium bubbles reach a critical size, they transform and grow unstably as voids, causing swelling. Helium on grain boundaries also promotes intergranular fracture by both fast crack propagation, at low to intermediate temperatures, and creep rupture at high temperatures.

It is well established that helium can be managed in NFAs, which contain a high density of Y-Ti-O NO. The NO trap helium in a high density of harmless nm-scale bubbles at the ferrite matrix interface [2]. Dual ion irradiations (DII) can be used to study helium behavior and related mechanisms in fusion relevant alloys. Heavy ions, such as Fe, are used to create displacement damage, while He ions are simultaneously injected to mimic n,α transmutation reactions [3]. The DII have shown that NFA with NO have a much larger number density of finer bubbles, compared to conventional 9Cr tempered martensitic steels [4–6].

The TEM has previously been used to show the association between NO and HB for a fraction of larger sizes in a population of NO [5, 7, 8], or for a single smaller NO [9]. Characterizing the general association between HB and a population of smaller NO is challenging in that it is generally not practically possible to find an imaging condition that can resolve both features at small sizes, except in special cases. Further, conventional TEM is also limited to imaging 2D projections of features in a 3D foil. Thus, for example, quantifying the relationship of HB and NO with angled grain boundaries is difficult.

New ET techniques seek to eliminate these limitations by taking a series of images over a wide range of tilt angles on a rotated cylindrical specimen. The tilt series can then be used to reconstruct a 3D representation of the microstructure, including HB. APT tips meet the cylindrical geometry requirement for ET, and then can be characterized by APT to observe the NO. Note while there are claims that APT can indirectly observe cavities, like HB, we have not found this to be the possible.

PROGRESS AND STATUS

Experimental Procedure

Materials and Irradiation Conditions

The NFA MA957, that contains a high density of NO, was DII at 500°C with 6.4 MeV Fe^{3+} and 1 MeV He^{+} ions in the DuET facility at the Institute of Advanced Energy of Kyoto University in Japan. MA957, which has been commonly used as a reference NFA, was first produced by INCO in the late 1970s [2]. The composition in wt.% of the heat studied here is; 13.6Cr, 0.30Mo, 0.98Ti, 0.26Y_2O_3, with trace impurities and the balance of Fe. The character and thermal stability of the NO in MA957, and their ability to refine the He bubble microstructure has been the subject of numerous studies [3–6, 10, 11].

The DII dpa and appm He as a function of depth in MA957, calculated using SRIM 2008, is shown in Figure 1. The APT TIPS were FIBed from liftouts taken from near the peak helium implanted damage region. The liftouts were mounted on a 5-post TEM grid and sharpened into APT tips using a 30 kV ion beam, followed by cleanup steps at 5 kV and 2 kV to minimize Ga contamination and damage. After cleanup, the tip of the APT needle was ~ 1 um from the original irradiated sample surface, nominally corresponding to ≈ 80 dpa and ≈ 4300 appm He.

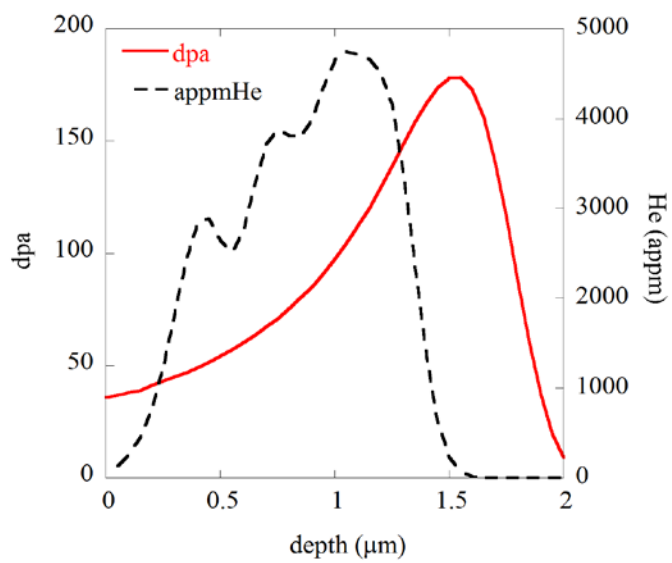

Figure 1. Depth profile of the DII dpa and He deposition calculated with the SRIM 2008 code.

Electron Tomography

A series of 140 bright field images were taken in a 200 keV FEI T20 Cryo TEM over a tilt range of -70° to +70° in 1° increments at a magnification of 50kx with an underfocus of 1um. While this defocus reduces the resolution of the images, the Fresnel white-black ring pattern improves the visibility of the bubble significantly. Simulation by Yao et al found that the optimum underfocus for imaging 1-3 nm bubbles is 750 nm, but 1μm is still near optimal [12]. The simulation suggested that the 1 μm underfocus results in a nominal bubble size that is ≈ 90% of its actual dimension. The series of images was then imported into a MATLAB code, using a custom weighted back projection algorithm that reconstructs the 140 ET data sets into a single 3D tomogram. Details of the reconstruction algorithm will be reported elsewhere.

Atom Probe Tomography

Following ET, the APT tip was run in a LEAP 3000x HR in voltage mode at 40K with a pulse fraction of 20%. The APT data was reconstructed using the CAMECA Instruments Integrated Visualization and Analysis Software (IVAS) 3.6.2 software. The TEM images of the specimen were used to determine the radius as a function of depth as input to the reconstruction. The [110] pole planes used in the reconstruction, were only visible in one region, because of a grain boundary in the center of the tip.

Correlative Tomography

The electron tomogram was imported into IVAS and the cluster analysis algorithm was used to determine the center of mass and size of both the HB and NO. The two datasets are initially reconstructed in separate arbitrary coordinate systems. The x, y, z coordinate systems were adjusted to align and overlay the HB and NO. An initial eyeball 3D overlay of the population HB and NO showed a 1:1 association. A refined overlay algorithm was then used to minimize the distance between the entire populations of correlated HB-NO pairs. Note because x, y, z adjustments were exactly the same for all off the HB and NO the statistical likelihood of false associations is virtually zero. Finally, the two datasets were imported into MATLAB for visualization.

Results

The 1 μm under focused bright field image of the DII MA957 in Figure 2 shows an extremely high density of 2-3 nm HB. No HB or NO is seen in the unirradiated control MA957 (not shown). The DII needle contained 3 grains, with one boundary roughly parallel and the other boundary roughly perpendicular to the tip axis. Two-dimensional projections of both the ET and APT tomograms are shown in Figure 3, for views parallel and perpendicular to the vertical grain boundary. Note the APT reconstruction volume is smaller than that for the ET. The grain boundaries can clearly be seen in the profile view parallel to the boundary planes. These results demonstrate the capability of ET to image and analyze HB. For example, the density of HB on the grain boundary is much higher than in the matrix and there is a ≈ 5 nm wide denuded zone on both sides of the horizontal boundary. Note a standard 2D TEM projection would not image the denuded zones unless the grain boundary was fully normal to the projection plane.

The superimposed ET and APT datasets is shown in Figure 4 where the red and blue isosurfaces represent the NO and HB, respectively. While in almost all cases, the surfaces of the bubbles and NO overlap, or are in close proximity, there are a few cases where there is clear separation between the two features. As seen in Figure 5, the center to center separations of HB and NO are larger at both the top and bottom of the tip. This is thought to be due to a slight miscalibration of either the APT reconstruction or the spatial superposition of the ET and APT, or both.

Future Work

While in a very preliminary stage, this work has shown for the first time on a large population of features, that there is a 1:1 correlation between HB and NO. A number of improvements will be pursued to further improve the quantitative correlation of the two techniques. Notably, improvements in the accuracy of APT reconstructions, both globally and locally, are constantly being made by the community. The combination of ET and APT also offer a way to further improve APT reconstructions. For example, trajectory aberrations associated with the local tip topology at an ET imaged void can be fully quantified in terms of the atom densities or local magnification factor. These experimental observables can be compared to and used to refine APT ion emission simulations. Further, future work will explore using additional information from both techniques to improve the individual correlation accuracy. For example, ET provides grain orientation information by local area diffraction measurements and real space images of other microstructures features, such as the grain boundaries, that can be tied to plane spacing and solute distributions measured in APT.

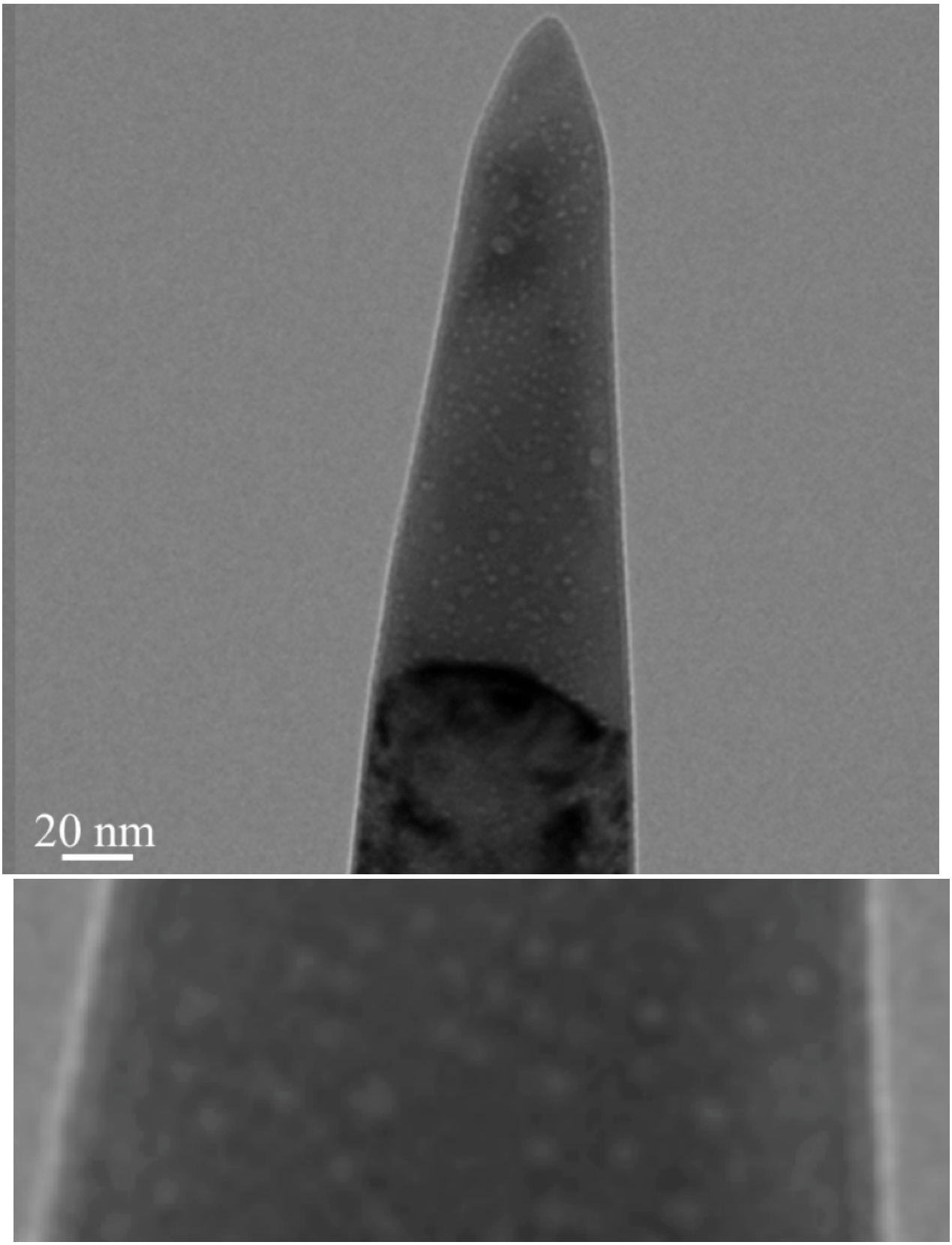

Figure 2. One of the 140 TEM bright field micrographs from the irradiated MA957 showing the size and Locations of HB. The lower figure is 5x time higher magnification.

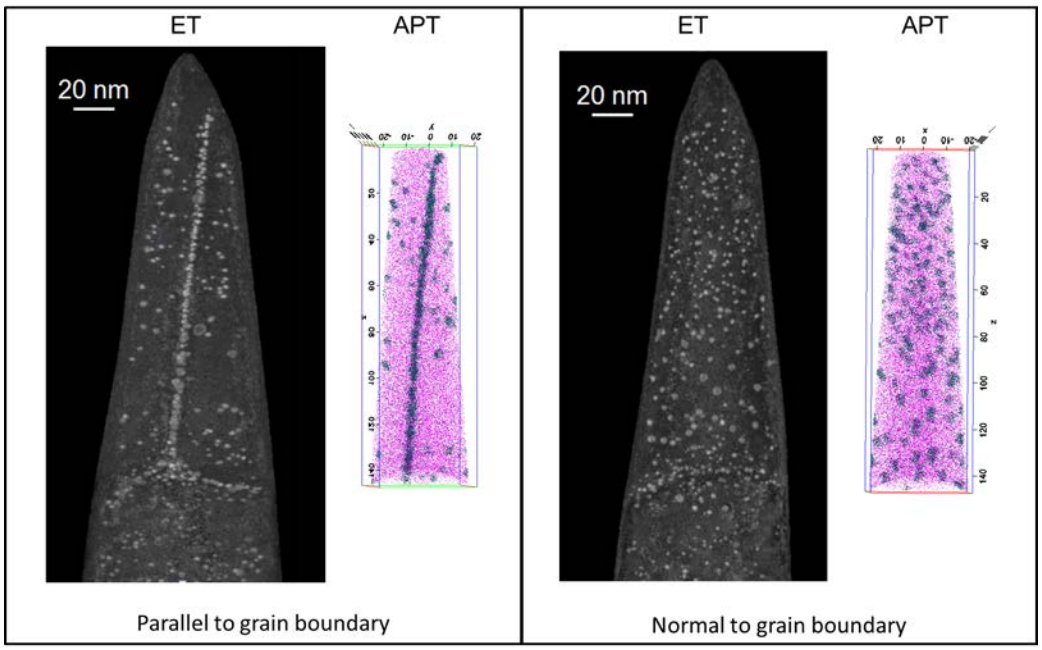

Figure 3. Two-dimensional projections of the ET and APT datasets parallel and normal to the grain boundaries. Note the volume of material in the APT reconstruction is smaller than the region imaged by ET.

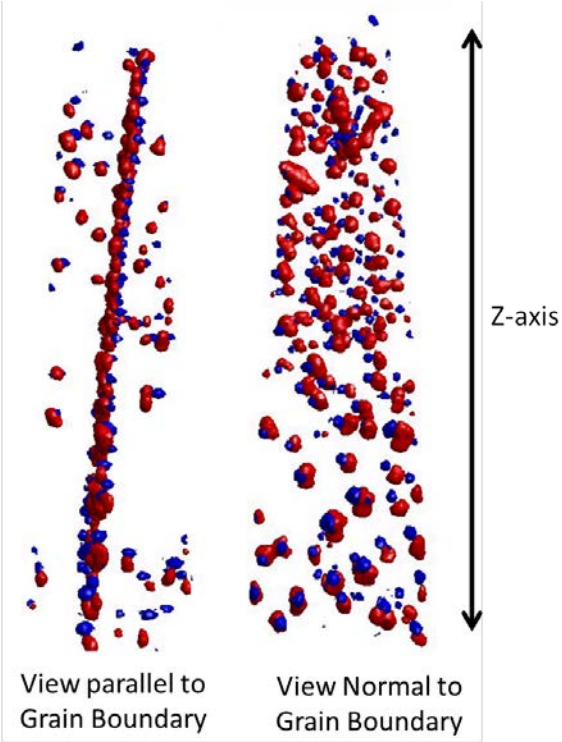

Figure 4. Projection views of the 3D correlated-superimposed ET and APT reconstructions parallel and normal to the grain boundaries showing the close association between the HB (blue) and NO (red) features.

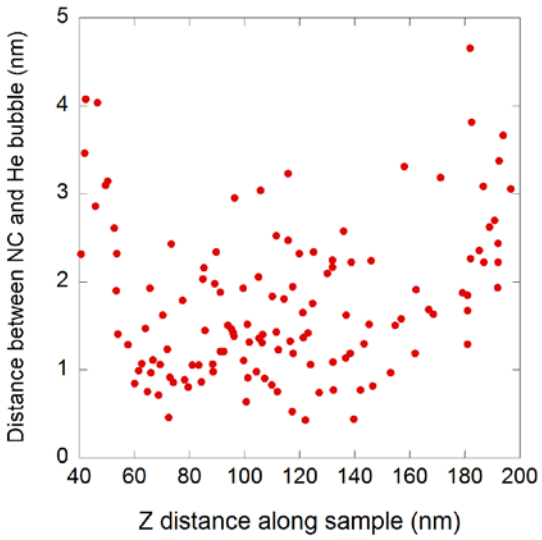

Figure 5. Center-to-center distances between the pairs of correlated NO and HB as a function of distance along the tip axis.

References

[1.] Zinkle SJ and Ghoniem NM. "Operating temperature windows for fusion reactor structural materials", *Fusion Eng. Des.* 2000;51-52(2000):55–71.

[2.] Odette GR, Alinger MJ and Wirth BD. "Recent Developments in Irradiation-Resistant Steels", *Annu. Rev. Mater. Res.* 2008;38(1):471–503.

[3.] Yamamoto T, Wu Y, Robert Odette G, Yabuuchi K, et al. "A dual ion irradiation study of helium-dpa interactions on cavity evolution in tempered martensitic steels and nanostructured ferritic alloys", *J. Nucl. Mater.* 2014;449(1-3):190–199.

[4.] Kurtz RJ, Alamo a., Lucon E, Huang Q, et al. "Recent progress toward development of reduced activation ferritic/martensitic steels for fusion structural applications", *J. Nucl. Mater.* 2009;386-388(C):411–417.

[5.] Yamamoto T, Odette GR, Miao P, Hoelzer DT, et al. "The transport and fate of helium in nanostructured ferritic alloys at fusion relevant He/dpa ratios and dpa rates", *J. Nucl. Mater.* 2007;367-370 A(SPEC. ISS.):399–410.

[6.] Kurtz RJ, Odette GR, Yamamoto T, Gelles DS, et al. "The transport and fate of helium in martensitic steels at fusion relevant He/dpa ratios and dpa rates", *J. Nucl. Mater.* 2007;367-370 A(SPEC. ISS.):417–422.

[7.] Odette GR, Miao P, Edwards DJ, Yamamoto T, et al. "Helium transport, fate and management in nanostructured ferritic alloys: In situ helium implanter studies", *J. Nucl. Mater.* 2011;417(1-3):1001–1004.

[8.] Chen J, Jung P, Hoffelner W and Ullmaier H. "Dislocation loops and bubbles in oxide dispersion strengthened ferritic steel after helium implantation under stress", *Acta Mater.* 2008;56(2):250–258.

[9.] Yutani K, Kishimoto H, Kasada R and Kimura a. "Evaluation of Helium effects on swelling behavior of oxide dispersion strengthened ferritic steels under ion irradiation", *J. Nucl. Mater.* 2007;367-370 A(SPEC. ISS.):423–427.

[10.] Cunningham N, Wu Y, Klingensmith D and Odette GR. "Materials Science & Engineering A On the remarkable thermal stability of nanostructured ferritic alloys", 2014;613:296–305.

[11.] Cunningham NJ. "Study of the Structure, Composition, and Stability of Y-Ti-O nm-Scale Features" [PhD Thesis]. University of California, Santa Barbara, 2012.

[12.] Yao B, Edwards DJ, Kurtz RJ, Odette GR, et al. "Multislice simulation of transmission electron microscopy imaging of helium bubbles in Fe", *J. Electron Microsc. (Tokyo).* 2012;61(6):393–400.